The effects of base steps and axisymmetry on supersonic jets over coanda surfaces

D. G. Gregory-Smith* and P. Seniort
School of Engineering, University of Durham, Durham, UK* and Asea Brown Boveri Research Centre, Baden, Switzerlandt

The effects of a base step in the exit plane of a slot on a supersonic jet blown over a convex coanda surface has been studied experimentally on a planar or two-dimensional model. An axisymmetric model has been used to study the effects of blowing radially outward over an axisymmetric coanda surface. Of particular interest is the jet structure and the conditions for the jet to break away from the surface. A complex flow field is revealed, with compression and expansion waves in the underexpanded core of the jet interacting with the outer free shear layer of the jet and with the boundary layer on the coanda surface, giving rise to separation bubbles on the surface. It is the growth and amalgamation of separation bubbles as the blowing pressure is increased that causes separation. The radial expansion effect with axisymmetry and the effect of a base step both enhance breakaway performance by reducing the shock cell length scale of the underexpanded jet and so reducing the size of separation bubbles. The direct application of this work was to the design of flares in the petroleum industry, but the work is also relevant to a wide range of coanda devices from blown jets for boundary-layer control to air movers and fluidic devices.

Keywords: coanda effect; curved wall jet; underexpanded jet; shock waves; axisymmetry; separation

1. Introduction

The coanda effect, whereby a jet of fluid attaches to a curved surface, has been studied for a considerable period. There are numerous applications of the coanda effect, varying from slot blowing for the control of boundary layers in the aerospace industry to small air movers, where it is used to move a large volume of air at low speed by entrainment from a high-pressure jet. The industrial impetus for this work was the development of high-pressure gas flares by British Petroleum plc. as described by Wilkins et al. (1977), one form of which is illustrated in Figure 1, which shows the axisymmetric model flare used in this work. High-pressure gas emerges from the slot at the base of the tulip-shaped body and flows around the convex surface, thereby entraining large quantities of ambient air, leading to efficient, smoke-free combustion. Usually the gas pressure is above that for choked flow and the jet is under-expanded. Of particular practical importance is the range of operation of the flare before the pressure becomes so high that the jet no longer adheres to the surface—a phenomenon termed *breakaway*. A related phenomenon, which we have termed *reversion*, occurs when a jet that has broken away follows the surface again. To achieve this, the blowing pressure has to be reduced considerably below the pressure that caused breakaway initially (i.e., there is a substantial hysteresis effect).

Address reprint requests to Dr. D. G. Gregory-Smith, at the School of Engineering, University of Durham, South Road, Durham, DH1 3LE, UK.

Received 1 September 1993; accepted 7 March 1994

© 1994 Butterworth–Heinemann

The important effects of curvature on the coanda jet have received wide attention, especially with respect to the turbulence structure and the entrainment (e.g., Bradshaw 1973, Alcaraz et al. 1977, Guitton and Newman 1977, Launder and Rodi 1981, Gregory-Smith and Hawkins 1991). However, most of this work has been concerned with high-speed jets, in which the series of expansion and compression waves in an underexpanded coanda jet form a complex flow pattern as they interact with the boundary layer on the surface, with the growing outer shear layer and with each other. Some experimental and theoretical work has been published for high-speed jets, such as Dash and Wolf (1984), Morrison and Gregory-Smith (1984), Green (1987), and Gregory-Smith and Gilchrist (1987). It is clear that the breakaway performance is determined by the interaction of the compression waves and the surface boundary layers. However, two important features of the actual flares have not been substantially addressed—the effect of a step between the slot exit and the curved surface, and the effect of the axisymmetric geometry. Both of these affect the breakaway performance and the jet structure.

The aim of this work, therefore, was to investigate the effects of base step and axisymmetry on the underexpanded jet flow structure and breakaway. This paper presents the results of two experimental investigations. The first was made using a planar or two-dimensional model with a variable base step, allowing good flow visualization using the techniques of interferometry, schlieren and shadowgraph. The second was on an axisymmetric model directly analogous to the full-sized flare. The experiments were restricted to air; no combustible gas was used with the models. Some limited work was carried out on a full-scale flare with natural gas, using shadowgraph and surface

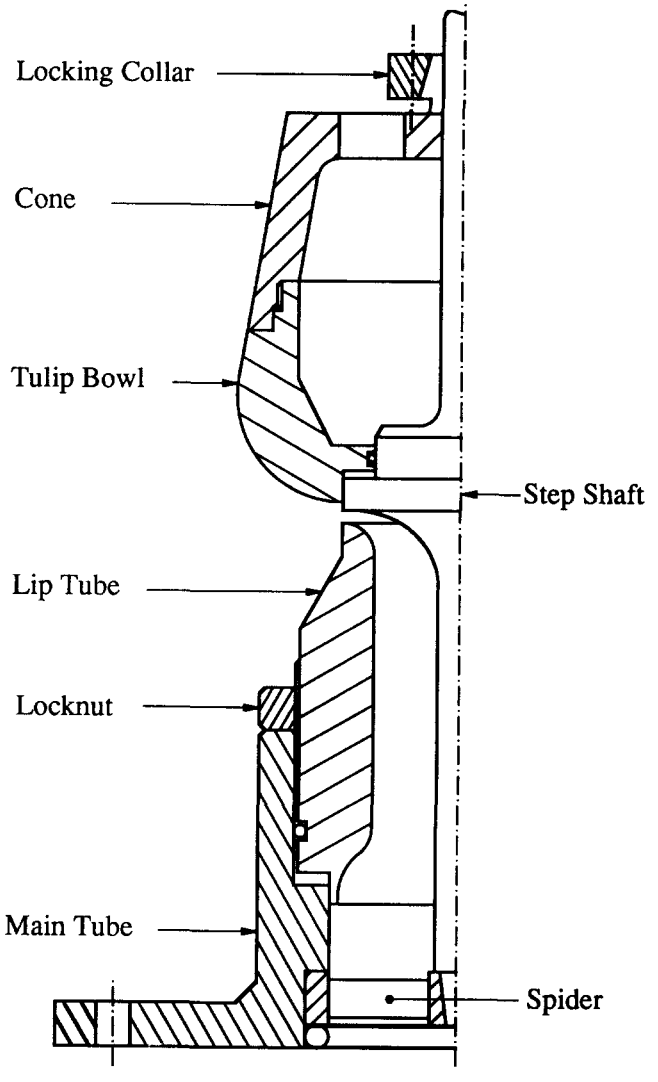

Figure 1 Axisymmetric flare model

flow visualization. It is intended that a companion paper (Senior and Gregory-Smith 1994), will be published presenting the results of computational work, which will supplement the work presented here.

A large number of combinations of slot height and step height were investigated for both the planar and axisymmetric models using the various techniques described in the following paragraphs. Of necessity, a restricted selection is presented here. Further details are given by Senior (1991).

2. Experimental method

The air supply to the apparatus from an air main at 35bar passed through a pressure control valve, two filters (to ensure clean air) and a second pressure control valve before entering the rig. The axisymmetric model is shown in Figure 1. The central shaft was designed as a register and a support member for the model, since this allowed simple indepenent adjustment of slot height and step height. Pressure tappings were made by inserting brass clock bearings into drilled holes in the flare surface and machining these flush to the surface. The tappings were placed at 2° streamwise intervals over the curved surface and at 3.00mm intervals on the conical section, with a spread over a 120° sector in the circumferential direction. The planar model was similarly constructed, but with optical glass sidewalls to allow the optical flow visualization.

The optical arrangement for the interferometry, schlieren and shadowgraph is described in detail by Gregory-Smith et al. (1990). A small laser was used for the interferometry and a pulsed xenon source was used for the schlieren and shadowgraph, allowing either continuous or spark images. The arrangement was a Z-type configuration, similar to that used for conventional schlieren. The planar model allowed good-quality photographs to be obtained using all three methods. The photographs obtained for the interferometry were digitized and quantitative results produced for Mach number and pressure fields. The schlieren and shadowgraph were used for qualitative analysis of the flow structure. Only schlieren and shadowgraph were used with the axisymmetric model because of the complication introduced by the axisymmetry.

Surface flow visualization was also used with both models to study areas of boundary-layer separation. A mixture of fluorescent pigment and a high-viscosity silicone oil was painted on to the surface. With the rig running, photographs were taken under ultra violet light. These could then be studied in relation to the static pressure distributions obtained from the tappings to gain a good understanding of the surface flow. With the planar model, the extent of the influence of the sidewalls could be seen from the surface flow visualization.

The identification of the points of breakaway and reversion was carried out carefully, since these are both features of a flow instability. Tests were made to establish the repeatability of the results and small disturbances such as mechanical vibration were also introduced to reveal the level of sensitivity. The partial reversion phenomenon described later was found particularly difficult to identify, but the other phenomena were quite well defined, even when these disturbances were applied.

With the field tests, only shadowgraph and surface flow visualization were attempted, in view of the practical restrictions of operating in daylight, ease of access and safety. Natural gas was used, mainly methane, and the shadowgraph was achieved using a 500 W slide projector set at its longest range, which gave a reasonable transmission shadowgraph. This was recorded using both still camera and *cine*cameras. For the surface flow visualization, the best mixture was found by mixing white titanium dioxide powder with the high-viscosity silicone fluid.

The rig operating conditions are defined in terms of the slot height and base step height, expressed as a ratio of the coanda surface radius of curvature and the upstream blowing pressure. This is expressed as a pressure ratio coefficient

$$C_{po} = p_{atm}/p_o$$

where p_{atm} is the downstream (atmospheric) pressure and p_o is

Notation

C_p	Surface static pressure coefficient $[(p - p_{atm})/(p_o - p_{atm})]$	p	Static pressure
C_{po}	Blowing pressure ratio coefficient $[p_{atm}/p_o]$	p_{atm}	Downstream, atmospheric pressure
		p_o	Upstream stagnation pressure

the upstream stagnation pressure, so that a high-blowing pressure gives a low value of C_{po}. The surface static pressures are also expressed as a coefficient defined by

$$C_p = (p - p_{atm})/(p_o - p_{atm})$$

3. Planar model results

3.1. Flow field structure

In order to discuss in detail the stepped, planar model flow field, a case with a slot height/radius ratio of 0.133 and a step ratio of 0.125 has been chosen. Senior (1991) shows a full range of results. Figure 2 shows a spark schlieren photograph with a vertical (i.e., parallel to the model axis) knife edge at $C_{po} = 0.191$, just before breakaway. Starting inside the nozzle, there are small disturbances on the lip surface, most probably due to separation of the boundary layer. Since these disturbances fail to propagate through the expression fans, their effect on the flow field appears to be negligible. At the nozzle exit, the two expansion fans at lip and step are clearly visible, along with evidence for accompanying lip shocks, which although quite weak (to judge by their interaction with the reattachment shock) nevertheless penetrate a considerable distance downstream into the jet core. Both the inner and outer shear layers thicken quite rapidly. At the attachment point of the inner shear layer, a turning shock is produced in the jet core. This exhibits noticeable curvature as it travels toward the jet edge and interacts with the incoming expansion from the lip and the compression wave resulting from the reflection of the step expansion at the outer jet edge. The next significant features are a separation shock at the coanda surface and, almost immediately opposite on the outer edge of the jet, the reflection of the step attachment shock as a strong expansion. The separation and its associated shock appear to arise from the influence propagating upstream of the strong compression wave that results from the first reflection of the step expansion fan. This wave is again reflected from the separation bubble as an expansion, which is made clearer further downstream where it undergoes another reflection from the outer jet edge as a diffuse compression zone. A second separation bubble appears to be a direct result of this second, incoming compression. Between these two separations, the strong incoming expansion (resulting from the reflection of the step-zone shock mentioned above) terminates the first separation bubble and generates another outward-traveling reattachment shock. Further downstream, the second reattachment shock, reflected from the jet edge as an expansion, ends the second separation bubble in an analogous manner to the reattachment after the first separation. By the end of the second separation, it appears that the outer shear layer growth largely eliminates the cell-like structure of the jet (which accords well with the surface pressure distribution; see the following).

This flow field pattern may be contrasted with that for no step, such as shown by Gregory-Smith and Gilchrist (1987) and confirmed by this work (see the interferogram, Figure 3). Their Figure 12, for instance, shows the expansion fan from the lip being reflected first from the coanda surface and then from the outer boundary of the jet as a compression wave traveling inward. This results in a gross separation that extends some 60° around the surface. The separation shock and the reflection of the incoming compression wave at the recirculation bubble are reflected from the outer shear layer as expansion waves and these eventually terminate the separation bubble. The most significant difference with the step present is the strong incoming expansion waves resulting from the reflection of the step-zone shock, which causes much earlier reattachment of the separation bubble.

3.2. Interferometry

Figure 3 shows an interferogram at $C_{po} = 0.303$ for the model with zero steps. It is apparent that the turbulent outer shear layer quickly obscures the fringe detail as the jet proceeds downstream. This allowed digitization of the interferogram

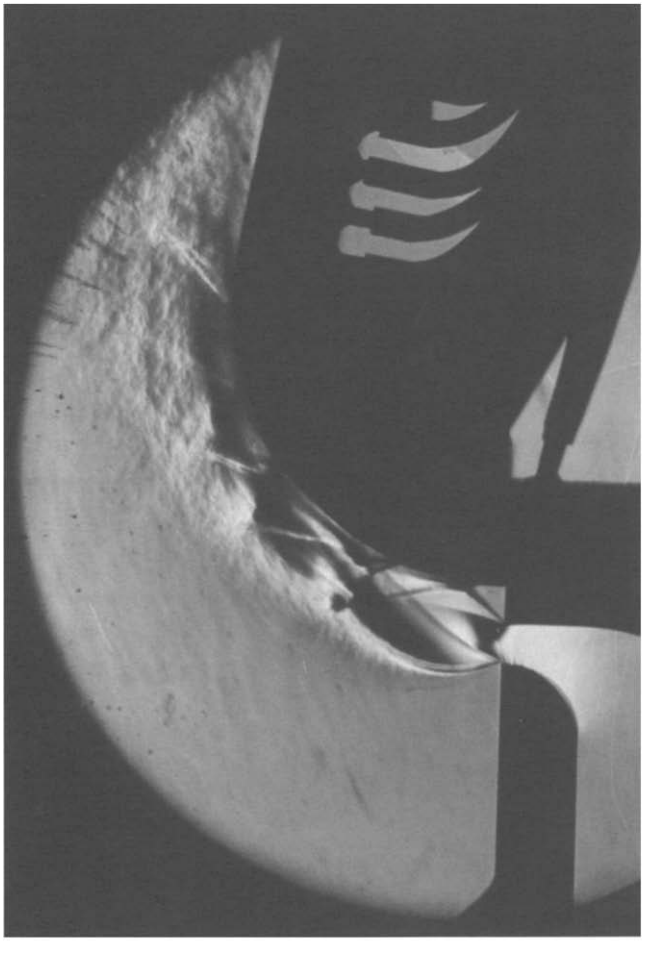

Figure 2 Planar model, spark schlieren near breakaway

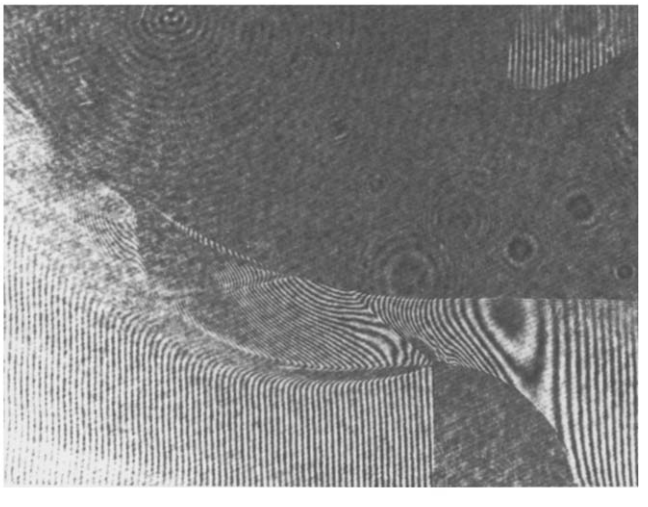

Figure 3 Planar model, interferogram

only for about the first 30° around the coanda surface. In addition, the bending of the working beam by the compression wave causes a shadowgraph that obscures the fringe pattern in the downstream half of the first cell. In fact, this was about the lowest value of C_{po} (highest blowing pressure) that useful interferograms could be obtained with zero step. For the stepped jet, the problem becomes much worse, even at modest blowing pressures, so that only the zero-step interferograms were analyzed.

The Mach number contours obtained from the digitized interferogram are shown in Figure 4. The sonic line lies inside the nozzle and confirms that the disturbances noticed in Figure 2 can be explained by supersonic flow/boundary-layer interaction. Although the pressure contours are not shown here, the rising Mach number indicates a favorable pressure gradient on the nozzle's upper surface, continuing onto the coanda surface under the influence of the lip expansion. This is terminated by the separation bubble, most clearly seen in Figure 3, and its associated sharp compression wave. The pressure in the separation bubble is substantially constant as would be expected for a low-speed recirculation zone. The pressure distribution obtained from the interferograms agrees very well with the values measured by the pressure tappings, as given by Gregory-Smith et al. (1990).

3.3. Surface pressure measurements

The surface pressure measurements aid the understanding of the boundary-layer behavior, since separation effects can be detected where these are too small for visualization. With zero-step height (Figure 5 for 0.133 slot/radius ratio) at a modest blowing pressure, $C_{po} = 0.496$, the wave pressure structure is smooth and regular, implying a fully attached boundary layer all along the coanda surface. As the blowing

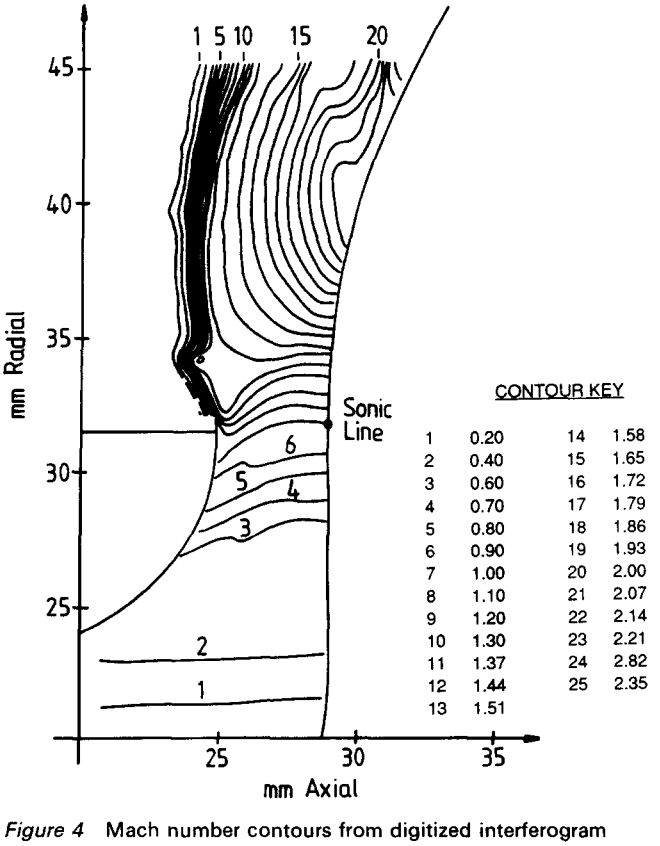

Figure 4 Mach number contours from digitized interferogram

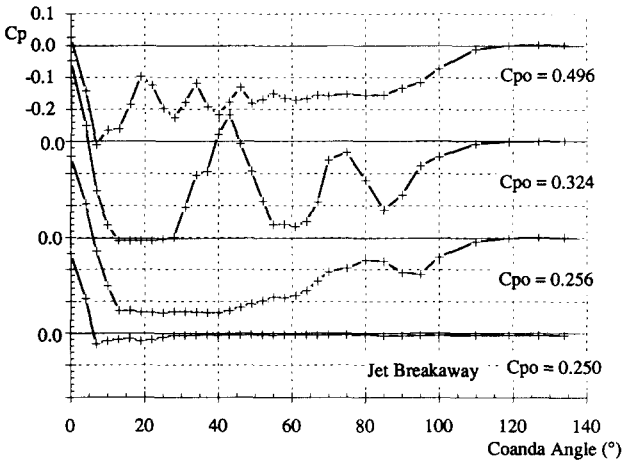

Figure 5 Planar model surface pressures, slot/radius = 0.133, no step

pressure increases (lowering C_{po}), evidence of separation at the first two troughs becomes clear—roughly constant pressure zones, indicating separation, extend upstream into regions that should have a favorable pressure gradient. Figure 5 also demonstrates the lengthening of the shock cell structure with a decreasing pressure ratio. Regions of strong pressure gradient appear after each separation, indicating reattachment. At a still lower pressure ratio, $C_{po} = 0.256$, the separations at the troughs of the first two waves have amalgamated and the reattachment has become weak, as shown by the small pressure rise of the first peak. Finally, at $C_{po} = 0.250$, the jet has broken away, as the failure to reattach allows air at atmospheric pressure to be drawn into the separation bubble causing the jet to flip away from the surface.

The presence of the step causes a very different pressure distribution to be produced, as can be seen in Figure 6, which is for a slot/radius ratio of 0.133 and a step height/radius ratio of 0.050. Subatmospheric pressure is seen in the step recirculation zone and the pressure oscillations are damped down by the interference of the expansion waves generated at the step edge and the reattachment shock at the end of the step recirculation zone. The cell structure approaches that of a free jet more closely and, so, the cell length is reduced (a plane free jet is half the scale of the equivalent plane wall jet). The pressure peaks are smaller and so the adverse pressure gradients are weakened. At the highest pressure ratio (just below that for

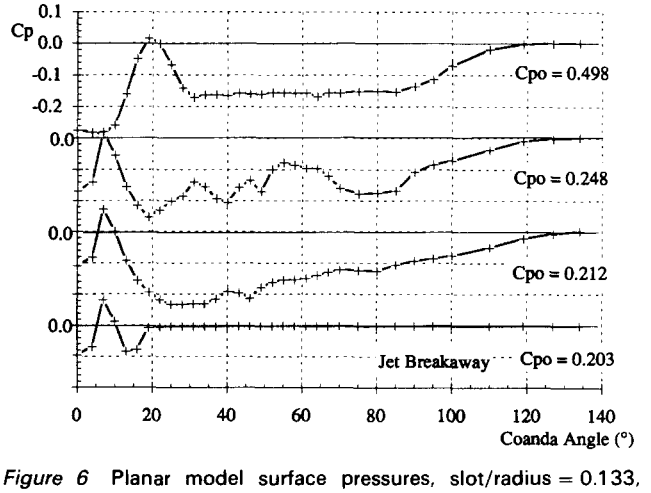

Figure 6 Planar model surface pressures, slot/radius = 0.133, step/radius = 0.050

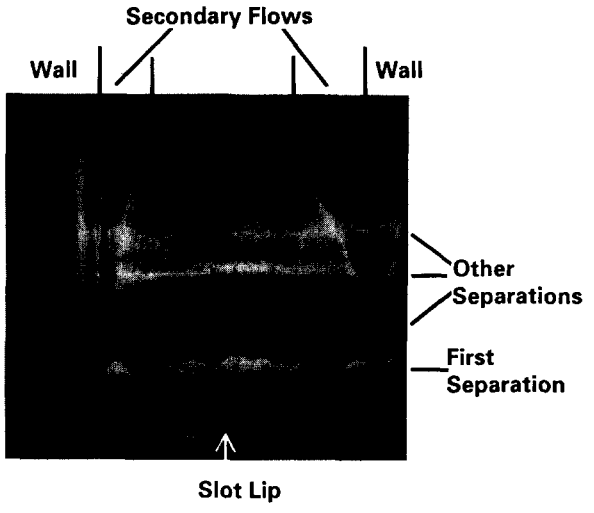

Figure 7 Planar model, surface flow visualization

choked flow), the pressure oscillations disappear after the first peak. Significant separation is not seen until near breakaway and this separation starts much further around the coanda surface (~25°) compared to the zero-stepped case (~12°) shown in Figure 7. The value of C_{po} is much lower for breakaway. However, near breakaway, the stepped case is similar to the zero-stepped case in that the pressure oscillations after the separation are nearly replaced by a gradually rising pressure. After breakaway, the jet still has a significant region of attachment to the coanda surface (nearly 20°) and this causes a noticeable upward deflection of the broken away jet, unlike the zero-step case.

3.4. Surface flow visualization

An example of the surface flow visualization is shown in Figure 7, which is for zero step, a slot/radius ratio of 0.133 and $C_{po} = 0.324$. The large accumulation of the oil and dye in the first separation is apparent, extending between 12° to 22° around the surface. A cross-stream variation is seen, but it is much less at the upstream (separation) edge than at the downstream edge, suggesting that secondary flows within the separated region may be responsible. Two thin stripes are also seen at about 70° and 90°, indicating further separations downstream that correspond to the pressure-tapping data (Figure 5). The last stripe corresponds to the end of the curved section and the start of the plane surface at 100°. However, the separations seem somewhat larger than those indicated by the pressure tappings and the oil itself may be affecting the flow slightly.

The secondary flows caused by the presence of the sidewalls are clearly seen in Figure 7. The main jet is narrowed and the extent of the separations sideways is reduced. However, some 80 percent of the cross section remains approximately uniform by the end of the curved surface and the surface pressure tappings continue to lie within this zone. This gives some confidence that the optical flow visualization and the surface pressures gave results fairly close to the two-dimensional form.

With a step present (not shown here), the step recirculation zone may be clearly seen, followed by a series of separation bands, again corresponding to the pressure troughs given by the surface tappings (Figure 6). That Figure 6 does not clearly indicate separations may be due to their small extent and/or to an influence of the presence of the oil. Although not shown here, as the blowing pressure rises, the number of bands decreases, with the pressure fluctuations increasing in wavelength.

3.5. Breakaway and reversion tests

The model was tested over the full range of slot/step combinations. The results in Figure 8 for breakaway shows the same trend as Gilchrist (1985) (see also Gregory-Smith and Gilchrist 1987), in that the breakaway pressure rises as the slot height is reduced—the important parameter being the slot height-to-coanda radius ratio. The breakaway pressures for zero step are slightly higher than Gilchrist's probably because the discontinuity at the step plate/coanda surface may cause transition (or at least additional turbulence) of the boundary layer. With a step, the effect of slot follows the same trend, but the dependence on slot height is stronger as the step is increased. At a given slot height, increasing the step increases the breakaway pressure, but to a decreasing extent so that the smallest step has the biggest incremental effect.

The reversion characteristics are shown in Figure 9. The lower pressure required for reversion is indicative of the hysteresis effect mentioned earlier. There is a stronger dependence on the presence of the step, with more improvement for breakaway. The flow visualization and static pressure-tapping results show that the step recirculation zone is maintained on breakaway. It appears that this provides the initial bulk turning of the flow and a recirculation shear layer that scales with step size. Both of these features tend to aid the entrainment or Chilowski effect (Bradshaw 1973) over the coanda surface and so promote reversion. Tests on the stepped flare with slot/radius ratios of 0.133 and 0.200 revealed a third type of behavior, partial reversion, in which the broken away jet

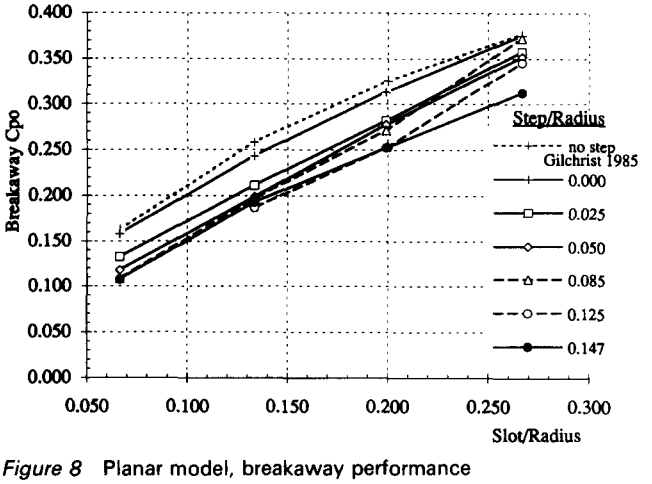

Figure 8 Planar model, breakaway performance

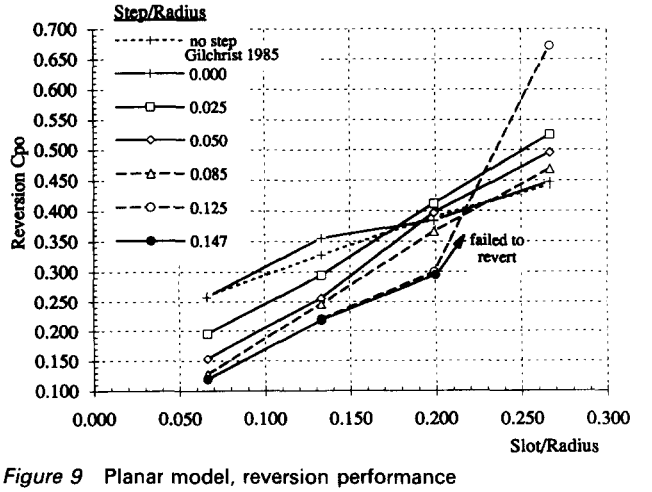

Figure 9 Planar model, reversion performance

was deflected back toward the coanda surface at approximately 45° to the vertical.

4. Axisymmetric model results

4.1. Flow field structure

Even with a shadowgraph or schlieren system well focused on a central plane, the finite depth of field will reveal noncentral features. This tends to confuse the picture for an axisymmetric flow field, since the off-central flow field is offset relative to the plane under investigation. Thus care has to be taken in the interpretation of the results, and comparison between different types of visualization may be necessary to obtain a reliable description of the flow. (It is not possible to present all the evidence in this paper.)

Figure 10 shows a schlieren photograph with a horizontal knife edge for a slot/radius ratio of 0.067. The value of $C_{po} = 0.124$ is just before breakaway. In spite of a nominally zero step, a disturbance can be seen coming from the step location. There appears to be a large, pale band emanating from the impact of the lip expansion. However, the shadowgraph for this condition shows a very strong compression wave interaction at the jet edge, opposite a large, separated zone on the surface. The band may well be the axisymmetric effect of the projected interaction and its relative straightness supports this view. The outer shear layer appears to develop much more rapidly compared to the planar model, due to the greater surface area-to-volume ratio of the axisymmetric flow.

As with the planar model, the introduction of a step makes a radical difference to the flow field. Figure 11 shows the schlieren photograph for a slot/radius ratio of 0.067 and a step ratio of 0.050, again near breakaway. The major effect is clear; the massive separation seen for the zero-step case is much reduced in scale and is pushed downstream. The cell-length scale is reduced, resulting in weaker compression regions. This is similar to the effect of the step for the planar model although details are not so clearly visible.

4.2. Surface pressure measurements

The wavelike surface pressure curves for the axisymmetric flare are illustrated by Figure 12, which shows the results for the 0.067 slot/radius ratio with zero step. They are similar to those for the planar model seen in Figure 5. However, two changes may be noted. First, the expansion imposed by the radial outward flow partially replaced the low surface pressures as

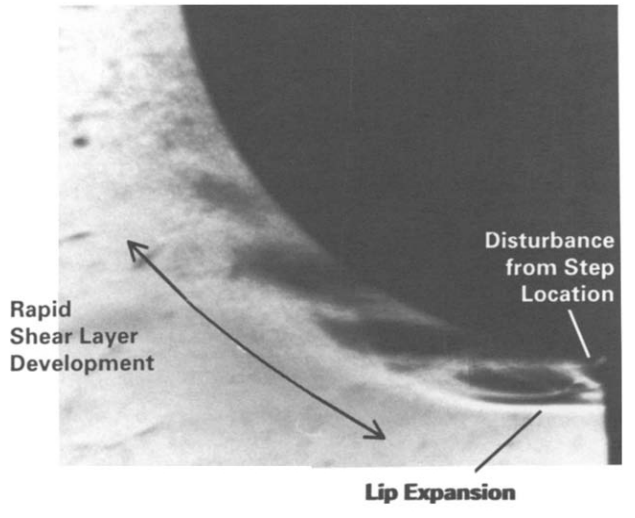

Figure 10 Axisymmetric model, schlieren, no step

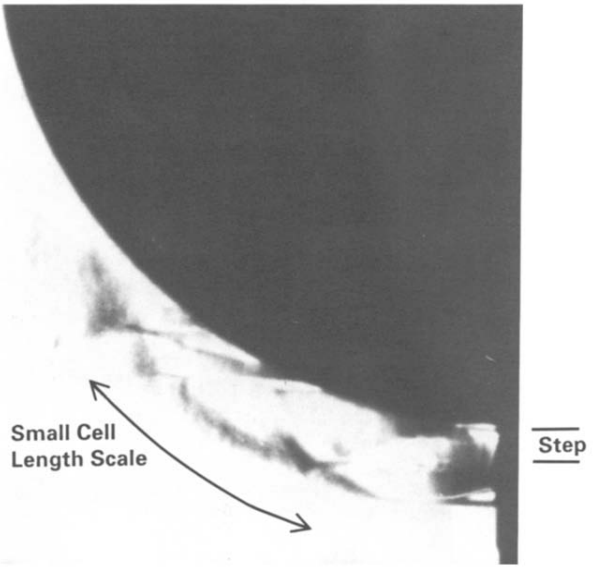

Figure 11 Axisymmetric model, schlieren, step/radius = 0.050

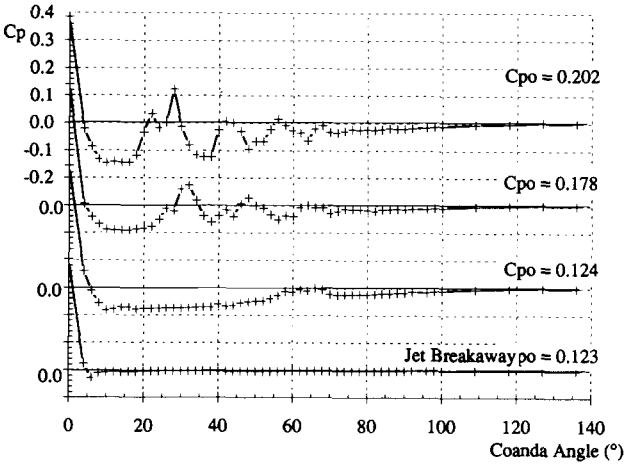

Figure 12 Axisymmetric model surface pressures, slot/radius = 0.067, no step

the turning influence (this effect being greater in the early part of the jet when the flow was more nearly radial). Second, the wave pattern was maintained until close to breakaway, similar to the planar stepped case (Figure 6). The mechanism of breakaway appears similar to the planar model, with the separation extending to about 60° just before breakaway and the flow then flipping off the surface as atmospheric air penetrates upstream.

The effect of a step/radius ratio of 0.050, Figure 13, is similar to that of a step on the planar model. In particular, the cell-length scale is reduced with smaller pressure peaks, the appearance of the separated region is delayed until higher blowing pressures, the separation is pushed downstream and the extent of the separation is reduced. The rig limitations prevented breakaway being reached for this step, but other geometries showed that the breakaway pressure distribution was again similar to the planar case, with the step expansion providing a region of attached flow to the coanda surface up to some 20°.

4.3. Surface flow visualization

The surface oil flow visualization results provide general confirmation of the interpretation of the other results, although

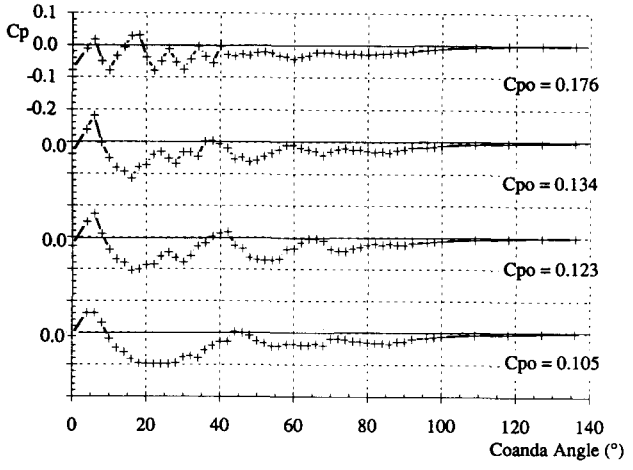

Figure 13 Axisymmetric model surface pressures, slot/radius = 0.067, step/radius = 0.050

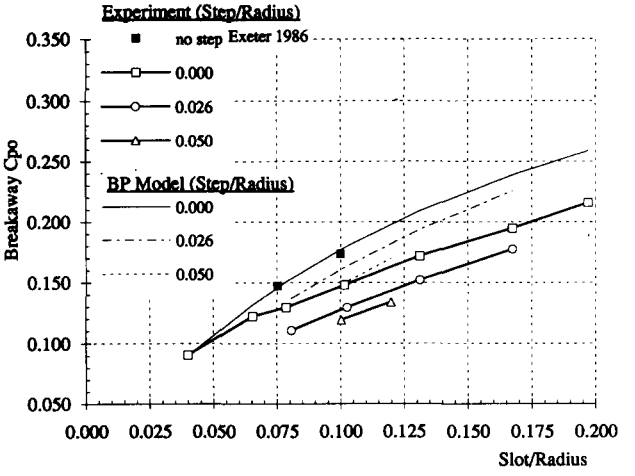

Figure 14 Axisymmetric model, breakaway performance

none of the photographs are presented here. The separated regions are identifiable by the accumulation of oil and their position accords well with the troughs in the pressure distributions. However, a feature not seen with the planar model is longitudinal streaks on the conical surface section that are spaced more or less regularly in the circumferential direction. These streaks have been seen on full-scale flares, where oil carried over with the combustible gas may be deposited on the flare surface. Some tests were carried out on a full-scale flare (with natural gas) using both surface flow visualization and shadowgraph. The longitudinal streaks were clearly visible, as were the separation bands on the coanda surface seen with the model flare. The cause of the streaks is not clear, but they may be due to longitudinal Görtler-like vortices generated in the unstable velocity profiles.

4.4. Breakaway and reversion tests

Due to the greater resistance to breakaway of the axisymmetric model, the air supply limited the configurations at which breakaway could be reached. This is clear in Figure 14, which shows the breakaway performance rising with reduced slot height and with the introduction of a step, as with the planar model. The reversion characteristics (not shown) respond in a similar manner. Comparative data from Green (1987) at Exeter University for an unstepped axisymmetric model is also shown, along with data converted from a correlation of full-scale methane results from British Petroleum (1980). Both sets for no step put breakaway at a lower blowing pressure than with this model, which may be due to the effect of the discontinuity (noted in Figure 10) increasing performance, as for the planar model. Differences in the nozzle exit flow may also have had an effect in this axisymmetric case, since the model was specifically designed to avoid disturbances in the nozzle. Such disturbances were noted in Green's rig and may be expected in the full-scale flare, which had only a rudimentary nozzle form. However, the general pattern is similar for all the results.

5. Discussion

The experimental work on breakaway and reversion demonstrates that these phenomena were repeatable within a small range of blowing pressure. This suggests that both are controlled by large-scale events, especially in the case of breakaway, although the slight sensitivity of reversion implies that turbulence plays a greater role in determining the lower limit of the hysteresis region. Considering the mechanism of breakaway, first for the unstepped planar model, the cell structure approximates that of a free jet with its center line as the curved wall. Two separation bubbles appear on the surface due to the interaction of compression waves or shocks with the boundary layer. As breakaway is approached, these bubbles grow and, at a critical value of C_{po}, amalgamate. The increase in the size of the joint bubble results in the recirculation velocity driven by the mainstream flow dropping and the reattachment point moving downstream. Both these factors raise the static pressure in the bubble and the jet rapidly flips off the surface. The evidence for the separation bubbles is provided by the optical and surface flow visualizations and the surface pressure measurements. The phenomenon of partial reattachment indicates that a stable flow is possible with the second bubble open to the atmosphere and with the first bubble closed. It is postulated that the joining of the two bubbles must occur before breakaway takes place. Reversion takes place primarily when the mild pressure drop caused by entrainment of the free jet close to the surface is able to bend the jet with its reduced momentum as C_{po} is increased. The edge of the inner shear layer approaches the wall and seals off a bubble from the near atmospheric pressure downstream. The pressure in the bubble reduces rapidly due to the entrainment/recirculation and the jet is sucked on the wall in a classic demonstration of the Chilowski effect (Bradshaw 1973).

The primary effect of the introduction of a base step is that the jet structure now scales more like that of a free jet with thickness the same as the slot height. This is achieved by the complexity resulting from the step expansion and the attachment shock at the end of the step recirculation zone. The separation bubbles are consequently smaller and more numerous, and the results suggest that the second and third bubbles amalgamate before the first bubble joins them to cause breakaway. Thus, the basic mechanism of breakaway is the same as for the unstepped case, although occurring at a higher blowing pressure. The broken away jet still has an expansion at the step edge, resulting in attachment of the jet for a significant angle on the coanda surface. Thus, the Chilowski effect described earlier achieves reversion at a much higher blowing pressure than for the unstepped flare. It is suggested that this strong Chilowski effect close to the slot permits local reattachment for some step configurations at a jet momentum too high to allow complete reversion, thus giving rise to the phenomenon of partial reversion.

Overall, the flow structures for axisymmetric and planar models are similar, and thus the planar model, which is much easier to study (the three-dimensional effects caused by the sidewalls do not affect the flow too much), is very helpful in

understanding the axisymmetric flow. However, the addition of radial expression reduces the cell-length scale and hence reduces the size of the separation bubbles and retards the amalgamation sequence leading to breakaway. Although the range of configurations covered was limited, the general trend of the breakaway results is similar to those for the planar model. However, the decreasing improvement in performance as step size is increased is less marked. This corresponds well to the shorter bubble lengths in axisymmetric flow, since these give more space for growth with step height before breakaway improvements are reduced by the amalgamation of bubbles. The growth in size of the step recirculation zone is also less, thereby maintaining the bubble system at a greater distance from the higher pressure zone at the transition from the curved to conical surface.

As to the application of the axisymmetric model work to the full-scale flare, it appears that the general behavior with respect to slot and step height variation is the same and the limited flow visualization on the full-size flare confirmed that the flow mechanisms were similar. The effect of the Reynolds number, which is obviously very different, would be expected to be small with the generally high turbulent nature of the flow. Although the difference in gas properties (specific heat ratio and gas constant) is significant, it appears to have little effect on the qualitative nature of the flow. The British Petroleum (BP) correlation for the breakaway condition seems acceptable. The main difference between this model and that of the BP and Exeter University studies is in the design of the nozzle to minimize disturbances and separations before the lip edge. That this produces such a large effect is surprising in view of the insensitivity of the inviscid calculations of the jet to the initial conditions at slot exit (see the companion paper, Senior and Gregory-Smith 1994). There is a small disturbance for zero step with this model due to the discontinuity at the step plate, but, of course, this does not apply to the stepped cases. Thus, a possible avenue for the further optimization of flare performance may lie in the detailed investigation of the effect of nozzle geometry.

6. Conclusions

An experimental investigation of the performance of planar and axisymmetric, unstepped and stepped model flares has been carried out successfully, with some limited, full-scale work as well. The work covered breakaway and reversion tests, flow field and surface flow visualization, and surface pressure measurements. A complex flow field is revealed with compression and expansion waves in the underexpanded core of the jet interacting with the outer free shear layer of the jet and with the boundary layer on the coanda surface, giving rise to separation bubbles on the surface. The results are substantially consistent between geometries and show that the basic mechanism of separation is the same, namely the growth and amalgamation of separation bubbles under the influence of increasing adverse pressure gradients as the blowing pressure is increased, thus reducing the pressure on the surface and allowing the jet to flip off the surface. The radial expansion effect with axisymmetry and the effect of a base step both enhance breakaway performance by reducing the shock cell-length scale of the underexpanded jet and so reducing the size of separation bubbles. The reversion mechanism is basically due to the Chilowski effect—the reduction of pressure close to the surface due to the jet entrainment becoming sufficient to cause the jet to reattach as the blowing pressure is reduced.

In terms of design improvements for flares, this work suggests that alteration of the surface profile to reduce adverse pressure gradients is unlikely to have much effect, since the breakaway is primarily due to the interaction of the various wave systems with the boundary layer. However, a possible line of investigation is that a surface discontinuity or second step might give rise to additional wave systems and so delay breakaway. Profiling the step cavity is unlikely to increase performance, as the work of Tanner (1988) suggests that this has minimal effect on the base pressure and hence on the external flow. As mentioned earlier, it is possible that internal nozzle profiling may yield some benefits.

It is clear that this work has applications to other coanda flow situations, in particular to external configurations (i.e., where the external pressure has a constant, here atmospheric, value). An important extension would be to internal coanda flows, such as air movers or BP's internal flare designs, where the jet blows radially inward at the entrance to a venturilike duct, thus entraining fluid and causing a pressure variation along the axis. It is probable that the jet structure near to the slot will be similar qualitatively to this work, but radially inward flow together with the axial pressure gradient will probably give a quantitatively different performance.

Acknowledgments

The authors gratefully acknowledge the support of British Petroleum plc., Kaldair Ltd. and the SERC for this work.

References

Alcaraz, E., Charnay, G. and Mathieu, J. 1977. Measurements in a wall jet over a convex surface. *The Physics of Fluids*, **20** (2), 203–210

Bradshaw, P. 1973. Effects of streamline curvature on turbulent flow. *AGARD-AG-169*

British Petroleum. 1980. Loss of coanda effect II. Private communication, BP Research, Sunbury-on-Thames

Dash, S.M., and Wolf, D.E. 1984. Interactive phenomena in supersonic jet mixing problems. Parts I and II. *A.I.A.A. Journal*, **22** (7), 903–916 and **22**(10), 1395–1404

Gilchrist, A. R. 1985. The development and breakaway of a compressible air jet with streamline curvature and its application to the coanda flare. Ph.D. Thesis, University of Durham, UK

Green, P. 1987. The fluid dynamics and aeroacoustics of external coanda flares. Ph.D. thesis, University of Exeter, UK

Gregory-Smith, D. G., and Gilchrist, A. R. 1987. The compressible coanda wall jet—an experimental study of jet structure and breakaway. *J. of Heat and Fluid Flow*, **8**(2), 156–164

Gregory-Smith, D. G., Gilchrist, A. R. and Senior, P. 1990. A combined system for the measurements of high-speed flow by interferometry, schlieren and shadowgraph. *Meas. Sci. Technol.*, **1**, 419–424

Gregory-Smith, D. G., and Hawkins, M. J. 1991. The development of an axisymmetric curved turbulent wall jet. *Int. J. Heat and Fluid Flow*, **12**(4), 323–330

Guitton, D. E. and Newman, B. G. 1977. Self-preserving turbulent wall jets over convex sufaces. *J. of Fluid Mechanics*, **81** (Part 1), 155–185

Launder, B. E. and Rodi, W. 1981. The turbulent wall jet. *Prog. Aerospace Sci.*, **19**, 81–128

Morrison, J. F. and Gregory-Smith, D. G. 1984. Calculation of an axisymmetric turbulent wall jet over a surface of convex curvature. *Int. J. Heat and Fluid Flow*, **5**(3), 139–148

Senior, P. 1991. The aerodynamics of curved jets and breakaway in coanda flares. Ph.D. Thesis, University of Durham, UK

Senior, P. and Gregory-Smith, D. G. 1994. The application of the method of characteristics to the investigation of supersonic jets over curved coanda surfaces. To be submitted to *Int. J. Heat and Fluid Flow*

Tanner, M. 1988. Base cavity at angles of incidence. *A.I.A.A. Journal*, **26**(3), 376–377

Wilkins, J., Witheridge, R. E., Desty, D. H., Mason, J. T. M. and Newby, N. 1977. The design development and performance of indair and mardair flares. *Off-shore Technology Conference* (Paper no. 2822) 123–130